# Local strain relaxation in $Si_{0.7}Ge_{0.3}$ on Si(001) induced by $Ga^+$ irradiation

Chinkyo Kim[a] and I. K. Robinson[b]
*Department of Physics, University of Illinois at Urbana-Champaign, 1110 West Green Street, Urbana, Illinois 61801*

T. Spila and J. E. Greene
*Department of Materials Science and Engineering, Coordinated Science Laboratory, and Materials Research Laboratory, University of Illinois at Urbana-Champaign, Urbana, Illinois 61801*

(Received 30 December 1997; accepted for publication 17 March 1998)

A strained pseudomorphic $Si_{0.7}Ge_{0.3}$ film grown by gas-source molecular-beam epitaxy on Si(001) was irradiated at room temperature with 25 keV $Ga^+$ ions. The gradual strain relaxation of the metastable $Si_{0.7}Ge_{0.3}$ film was monitored using *in situ* x-ray diffraction as a function of dose. Based on a dimensional argument, the ion-induced damage scales as extended defects. The Hendricks-Teller model was successfully applied to explain the shifting and broadening of the additional diffuse scattering. © *1998 American Institute of Physics.* [S0021-8979(98)05912-X]

## I. INTRODUCTION

$Si_{1-x}Ge_x$ has been one of the most extensively studied systems in thin film physics due to both scientific interest in its strain-induced phenomena and its technological applicability.[1–6] With a growing demand for multilayer structures, the main interest in this area lies in the growth of defect-free pseudomorphic films which are highly strained. However, theoretically predicted $Si_{1-x}Ge_x$ critical thicknesses do not concur with the values determined by experiments. It is believed that growth of $Si_{1-x}Ge_x$ is so dominated by kinetic effects that the energy of the film is not minimized at each growth state. It is found that the experimentally determined critical thickness of $Si_{1-x}Ge_x$ on Si substrates is much larger than that predicted by equilibrium theory. The region between the equilibrium critical thickness and the experimentally determined critical thickness is therefore metastable.[7,8] We expect that if a film is in the metastable regime, even though it is commensurate with the substrate, it might relax as perturbations or excitations are provided, such as irradiation, which would move the system towards the energy minimized state.

The effect of post-growth high temperature thermal annealing on the strain relaxation of metastable $Si_{1-x}Ge_x$ thin films has been studied by many people.[9,10] The reason for this interest is that thermal annealing is a routine step in device processing and strain relaxation causes a dramatic change in the device characteristics. Sardela and Hansson[10] reported both in-plane and out-of-plane lattice relaxation due to thermal annealing $Si_{1-x}Ge_x$ on Si(001) as a function of temperature and composition using high resolution reciprocal lattice mapping. In their work, $Si_{1-x}Ge_x$ films were grown pseudomorphically within the metastable regime defined above. Misfit dislocations, activated by thermal annealing, were introduced giving rise to shifts in Bragg peak positions. Peak broadening, accompanied by a decrease in the peak intensity, was attributed to the increased mosaicity caused by misfit dislocations.

Ion implantation has long been used for doping semiconductors and it has many advantages, such as low temperature doping with minimal diffusion, the creation of shallow and well defined doping layers and the precise control of doping concentration, over other doping methods. However, it has a major shortcoming: it induces defects in the crystal. That fact has attracted many researchers to investigate irradiation effects in semiconductor materials either to ameliorate the problems caused by the defects or to study the strain relaxation induced by irradiation. Recent work on strain relaxation by irradiation of semiconductors including $Si_{1-x}Ge_x$ is described in Refs. 11–20. These studies can be summarized by two general properties of irradiation effects in crystalline materials: (1) the out-of-plane lattice constant expands due to point defects (such as interstitials) with virtually no change in the in-plane lattice constant and (2) crystal damage is removed by thermal annealing.

Our goal in this work was to investigate ion-irradiation-induced strain relaxation in a metastable $Si_{0.7}Ge_{0.3}$ film grown on Si(001). The experiments were carried out using 25 keV $Ga^+$ irradiation of a $Si_{0.7}Ge_{0.3}$ layer grown by gas-source molecular-beam epitaxy. Strain relaxation was measured as a function of ion dose using x-ray diffraction reciprocal lattice mapping (RLM) at the National Synchrotron Light Source (NSLS) at Brookhaven National Laboratory (BNL). The data were analyzed to provide both macroscopic relaxation using Bragg peak positions and microscopic relaxation deduced from the distribution of diffuse scattering near Bragg peaks. The latter is due to structural imperfections caused by increased mosaicity or local strain fields.

## II. EXPERIMENTAL PROCEDURE

A nominally 200-Å-thick $Si_{0.7}Ge_{0.3}$ film was grown pseudomorphically on Si(001) by gas-source molecular-beam epitaxy using $Si_2H_6$ and $Ge_2H_6$ at 500 °C.[21] The actual thickness was determined to be $240\pm5$ Å by Rutherford backscattering spectroscopy (RBS) and x-ray reflectivity.

[a]Present address: Opto-electric Group, LG Corporate Institute of Technology, 16 Woomyeon-dong, Seocho-gu, Seoul 137-140, Korea.
[b]Electronic mail: ikr@uiuc.edu

 

The Ge concentration was found by high resolution x-ray RLM and RBS to be $29.5 \pm 0.3\%$. According to previous work, 240 Å at this composition should be in the metastable regime.[22,23]

*In situ* x-ray measurements during ion irradiation at room temperature were done at beamline X16A of the National Synchrotron Light Source at Brookhaven National Laboratory. A five-circle diffractometer combined with an ultrahigh vacuum chamber equipped with a $Ga^+$ ion source were utilized at the beam line. A double-crystal Si(111) monochromator was used to select 1.56 Å wavelength x rays. The scintillation detector had a 2 mm×2 mm slit and no analyzer crystal. Measurements were made in reciprocal space using the diffractometer control program SUPER. The sample was oriented with the (202) and (111) substrate peaks. To monitor the relaxation of the film due to irradiation, index scans in the $H$ and $L$ plane passing through the (202) peak of the film were done after each dose.

The $Ga^+$ ion-irradiation source was set to raster the entire sample. In high vacuum below $2\times10^{-7}$ Torr, the sample was irradiated with 25 keV $Ga^+$ ions at nearly normal incidence. This corresponds to a penetration depth of approximately 1000 Å in $Si_{0.7}Ge_{0.3}$ as determined using the TRIM computer simulation code. The energy of the $Ga^+$ ions was chosen to provide a relatively uniform defect concentration while depositing most of the ion energy in the substrate. The dose rate was approximately $1.5\times10^{12}$ (ions/min cm$^2$).

## III. EXPERIMENTAL RESULTS

X-ray diffraction data obtained during these experiments consist of two primary components: a sharp, coherent peak and a broad peak due to diffuse scattering. The sharp peak comes from coherent long-range structural order in the film imposed by the crystalline substrate. In contrast, the diffuse peak can have several sources: thermal vibration of atoms (phonons), short-range ordering, strain fields near dislocation cores, and point defects. Therefore, with increasing dose, we expect a decrease in the coherent peak intensity, with a possible peak shift, and an increase in diffuse scattering.

The experiments were carried out at room temperature. The sample remained aligned during the irradiation. Thus, the only variable is the ion dose so any change in diffuse scattering must result from local strain fields associated with either point defects or dislocations.

Figure 1 shows RLMs measured after different doses. The axis coordinates are in reciprocal lattice units (RLUs) of bulk Si. The SiGe film peak and that of the Si substrate are seen to be separated purely in the direction of the perpendicular momentum transfer index $L$, confirming pseudomorphic growth of the film. The RLM before dosing shows the typical broadening in the $L$ direction due to the finite thickness effects and a very narrow profile in the in-plane direction. Therefore, it can be inferred from the RLM that the as-grown film is commensurate with no dislocations within the limit of our experimental resolution. The resolution ($\Delta a/a$, where $a$ is an in-plane lattice constant) for detecting changes in in-plane strain with our setup is $\simeq 5\times10^{-4}$ corresponding to a linear dislocation density of $5\times10^4$ cm$^{-1}$.

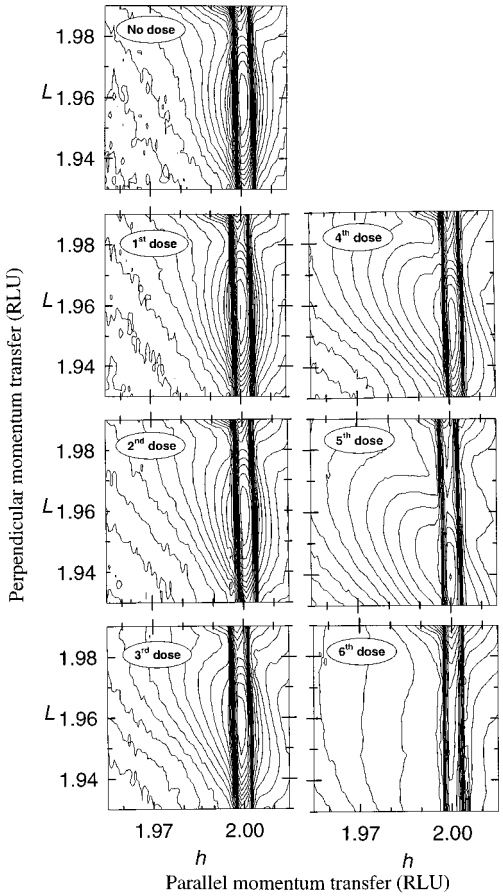


FIG. 1. Mesh scans of a 240-Å-thick $Si_{0.7}Ge_{0.3}$ sample grown on Si(001) and irradiated with 25 keV $Ga^+$ ions. Logarithmically spaced intensity contours are plotted near the Si(202) substrate Bragg peak as a function of $H$ along (100) and $L$ along (001) in substrate reciprocal lattice units. The accumulated doses are $8.0\times10^{10}$, $3.2\times10^{11}$, $1.0\times10^{12}$, $3.2\times10^{12}$, $1.4\times10^{13}$, and $3.6\times10^{13}$/cm$^2$, respectively.

The position of the SiGe(202) peak shifts in the out-of-plane direction with increasing dose. This is due to the dilation effect caused by ion-induced point defects mentioned above. However, this coherent (202) peak does not shift, within error, in the in-plane direction.

With increasing $Ga^+$ ion dose, an asymmetric diffuse peak starts to appear in Fig. 1 (more easily seen in Fig. 2 below) and grows in strength. This diffuse feature is broadest along the diagonal (101) direction, which is the direction corresponding to crystal mosaic. This suggests that the defects responsible give rise to strain fields that have shear character, rather than with changes of unit cell volume or compositional variations.[24–26] Even though it is difficult to see directly into the RLMs, it will be shown in the following analysis that this broadening is accompanied by a small peak shift toward a smaller $H$ value, which increases with dose.

Symmetric diffuse scattering associated with the Si substrate (202) peak is also partly seen in the upper region of the RLM. We observed no change of this diffuse scattering with dose. Furthermore, no time dependence of any feature in the data was seen over the course of the measurement, which was typically 3 h for each mesh scan.

For more quantitative analysis of strain relaxation, a set of scans along the in-plane $H$ direction passing through the

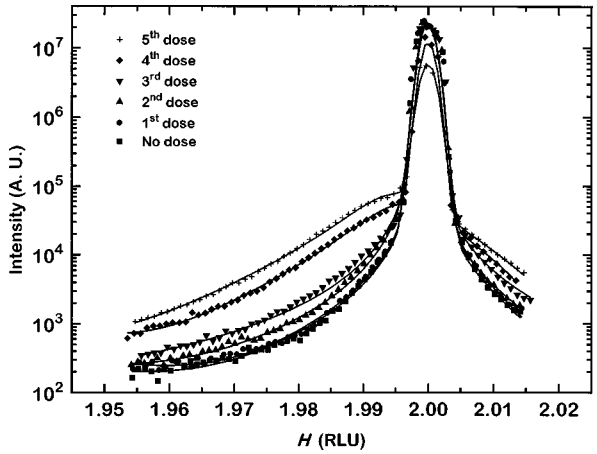


FIG. 2. Sections of data as a function of dose from Fig. 1. The cuts are along the $H$ direction, passing through the (202) peak of SiGe. After the sixth dose, since the film was amorphized was no peak found in the film.

(202) peak of the film was selected. The scan prior to the first dosing, in Fig. 2, shows symmetric diffuse scattering with a $1/q^2$ dependence, where q is the momentum transfer difference from the Bragg peak. This is likely due to Huang diffuse scattering[27,28] from residual defects as well as thermal diffuse scattering. The appearance and shift of the broad, diffuse peak with increased dose of $Ga^+$ ions are more clearly seen in Fig. 2. As a result of irradiation, the peak intensity of the coherent SiGe diffraction decreased and the intensity of diffuse scattering increased. For a clearer comparison, the diffuse scattering data are shown in Fig. 3 after subtraction of the scan from the unirradiated sample. The fits are Lorentzians, used to parametrize the data. Note that data near the coherent peak have been omitted in order to consider the diffuse scattering only.

Table I shows the film strain as a function of ion dose. The in-plane strain obtained from the diffuse peak is defined by $\varepsilon_{\parallel,\mathrm{diff}}=(a_d-a_f)/a_f$, where $a_d=2a_0/H_{\mathrm{diff}}$ is the in-plane lattice constant of the film determined by the diffuse peak position, $H_{\mathrm{diff}}$, in Fig. 3. $a_f$ is the lattice constant of the bulk $Si_{0.7}Ge_{0.3}$ alloy, which is 5.494 Å from Vegard's rule, and $a_0$

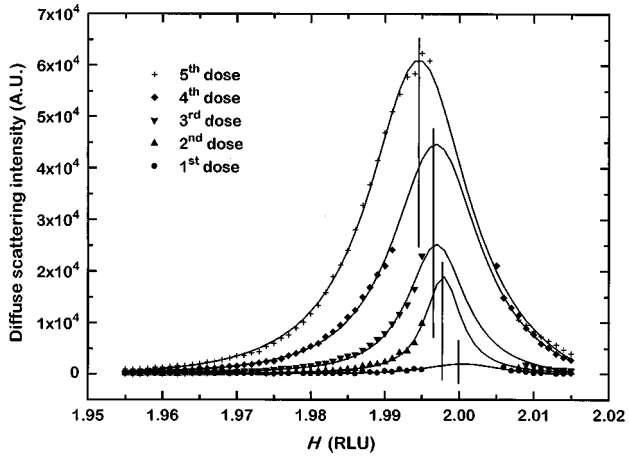


FIG. 3. Diffuse scattering component from Fig. 2 after subtraction of the zero-dose scan. Note that the coherent peak is not perfectly subtracted, and has been omitted. The fits are Lorentzians.

TABLE I. Accumulated doses on $Si_{0.7}Ge_{0.3}$ film and strains in the in-plane and perpendicular directions. The strains are based on the peak position in the RLMs of Fig. 1. They are relative to the fully relaxed lattice constant of $Si_{0.7}Ge_{0.3}$ obtained using Vegard's law. The errors in the strain determination are $\pm 0.0005$ for $\varepsilon_{\parallel,\mathrm{coh}}$, $\pm 0.001$ for $\varepsilon_{\parallel,\mathrm{diff}}$ and $\pm 0.0015$ for $\varepsilon_{\perp}$.

| | Accumulated dose (ions/cm$^2$) | $\varepsilon_{\parallel,\mathrm{coh}}$ | $\varepsilon_{\parallel,\mathrm{diff}}$ | $\varepsilon_{\perp}$ |
|---|---|---|---|---|
| Before dose | · | −0.0115 | ··· | 0.0097 |
| After 1st | $8.0\times10^{10}$ | −0.0114 | ··· | 0.0097 |
| After 2nd | $3.2\times10^{11}$ | −0.0115 | −0.0104 | 0.0093 |
| After 3rd | $1.0\times10^{12}$ | −0.0115 | −0.0100 | 0.0098 |
| After 4th | $3.2\times10^{12}$ | −0.0114 | −0.0099 | 0.0113 |
| After 5th | $1.4\times10^{13}$ | −0.0114 | −0.0088 | 0.0191 |
| After 6th | $3.6\times10^{13}$ | ··· | ··· | ··· |

is the lattice constant of Si, 5.431 Å. The coherent strains are defined by $\varepsilon_{\parallel,\mathrm{coh}}=(a_c-a_f)/a_f$ and $\varepsilon_{\perp}=(c_c-a_f)/a_f$, where $a_c$ and $c_c$ are the in-plane and out-of-plane film lattice constants determined from the measured Bragg peak positions. There is no significant change in the in-plane strain with dose, but the out-of-plane strain increases, as expected. Throughout the experiment, the film remains under strong compression in-plane and expanded out-of-plane because of the Poisson effect.

The shape of the diffuse scattering profiles, indicated by the position and full width at half maximum (FWHM) of the peaks, changes with dose. If defects are randomly distributed and the strain fields around the defects are independent and not overlapping, the FWHM and position of the diffuse peak associated with those strain fields would be constant with increasing dose as the defect concentration increases. The only effect would be an increase in peak intensity. Hence, in our case, the data indicate that the defect strain fields must overlap, and so cannot be independent of each other. As shown in the lower panel of Fig. 4(b), the FWHM and peak shift saturate after a certain amount of dose. These trends can be described reasonably well with exponential functions.

The peak position after the fifth dose is $H=1.994\pm0.002$ which corresponds to the lattice parameter we would expect for a fully relaxed film of $Si_{0.7}Ge_{0.3}$ estimated in the following way. First, we estimate the equilibrium critical thickness to be $h_C=153$ Å using the theory of Fischer *et al.*[29] This theory[29] goes beyond the usual balancing of strain energy with dislocation line tension by including the interactions between dislocations. Second, we estimate the lattice parameter of the 240 Å film, which, being slightly above the critical thickness, remains elastically strained to maintain mechanical equilibrium with the dislocations.[30] This calculation gives 5.454 Å and a peak position of $H=1.992$ which is slightly further shifted than what we saw after the fifth dose. Since the film became amorphized after the sixth dose, as indicated by the absence of a Bragg peak in Fig. 1, the amount of peak shift after the fifth dose was the maximum shift observed before amorphization.

## IV. DISCUSSION

To characterize the kind of defect present, we use a dimensional argument to scale the integrated intensity of the

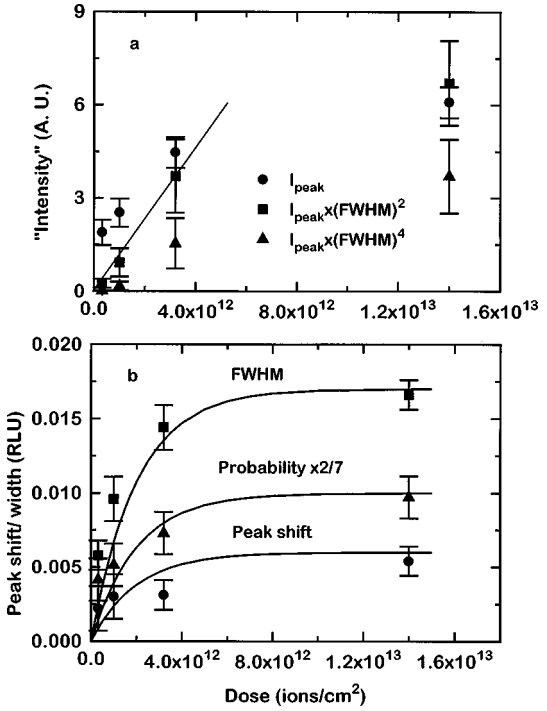


FIG. 4. Fitting parameters for Lorentzians and for the Hendricks-Teller model. In the upper panel, different scaling relationships are tested, with the best indicated by a straight line. The calculated values have been scaled to fit into one graph. In the bottom panel, the FWHM and peak shift were obtained from Lorentzian fits while the probability was obtained from the Hendricks-Teller model. The solid lines indicate an exponential relaxation with a characteristic dose of $2\times10^{12}$/cm$^2$, that serves as a guide to the eye.

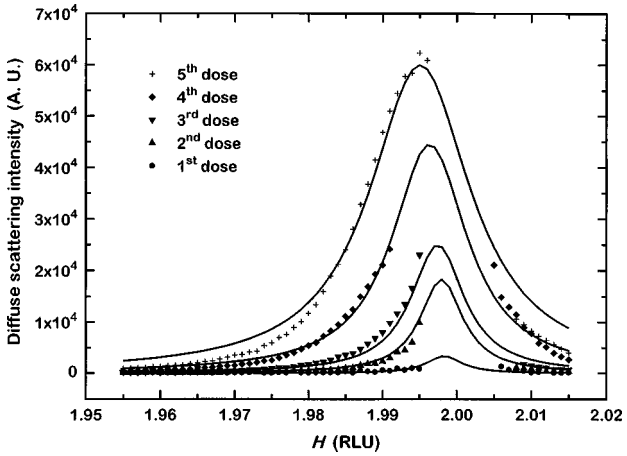


FIG. 5. The same data as in Fig. 3, but fitted using the Hendricks-Teller model. Two parameters in Eq. (2), defect density and peak height, have been adjusted for each data set.

diffuse peak.[31] Let us consider the case in which a point defect induces a three-dimensional (3D) strain field extending to a radius R. Since it depends on the number of atoms displaced by the strain field, the integrated intensity of the diffuse peak should be proportional to $N_{def}\cdot R^3$, where $N_{def}$ is the number of defects. This assumes that the strain field is caused by 3D point defects. Since R is determined by the reciprocal of the FWHM, the integrated intensity is proportional to $N_{def}\cdot FWHM^{-3}$. However, by definition, the integrated intensity is also proportional to $I_{peak}\cdot FWHM^3$, where $I_{peak}$ is the maximum of the intensity distribution, which extends an amount FWHM/2 in all three reciprocal space directions. Therefore, relating these two, we would expect that that $N_{def}$ would be proportional to $I_{peak}\cdot FWHM^6$ in the 3D case.

However, if R is larger than the film thickness, T, the vertical size of the defects is limited instead by the extent of the film. Then the dependence of $N_{def}$ on FWHM drops to the fourth power instead of the sixth since the FWHM in the surface normal direction would no longer change. If we repeat this argument for extended line defects instead of point defects, the integrated intensity varies as $N_{def}\cdot R^2$ for a thick sample and $N_{def}\cdot RT$ for a film of thickness T. In this case we obtain $N_{def}\propto I_{peak}\cdot FWHM^4$ for a thick film and $N_{def}\propto I_{peak}\cdot FWHM^2$ for a thin film where the range of the strain field is limited by the thickness. Other finite size effects that limit the size of the strain field would similarly reduce the power of FWHM appearing. We now consider what is seen in the data. For the first three doses in Fig. 4(a), the best scaling of the intensity with dose is $N_{def}\propto I_{peak}\cdot FWHM^2$. Therefore, based on the above dimensional arguments, the ion-irradiation damage detected in this experiment scales as extended line defects.

This interpretation is consistent with Kaganer *et al.*'s work.[32] They calculated the diffraction intensity strained AlAs/GaAs, $Si_{1-x}Ge_x$/Si and AlSb/GaAs heterostructures containing randomly distributed misfit dislocation networks and showed that the result was consistent with measurements. One of their conclusions was that, at a low dislocation density, the coherent diffracted and diffuse peaks are separated by a small amount, 0.0005 Å$^{-1}$. This kind of separation was only observable within a certain range of dislocation densities, around 700 cm$^{-1}$, because the coherent peak was found to decrease exponentially.

The role of dislocations at the interface is to relieve the strain of the epitaxial film by changing its lattice constant. So, relaxation upon introducing dislocations can be modeled by embedding unit cells with an increased lattice constant among the original lattice in a random way. This is conveniently achieved by the Hendricks-Teller model,[33] which provides the diffraction profile from a random sequence of two different unit cells of lengths $a_0$ and $a_1$ along one dimension. In our case, the unperturbed unit cell length is the Si lattice constant $a_0=5.431$ Å and $a_1$ will depend on the Burgers vector of the dislocation. The probability of finding a unit cell with a lattice constant $a_1$ at a certain lattice point is given by $P$. If $q$ is the momentum transfer, then the model defines an average phase $\phi$,

$$\tan\phi=\frac{(1-P)\sin(qa_0)+P\sin(qa_1)}{(1-P)\cos(qa_0)+P\cos(qa_1)}. \tag{1}$$

The diffracted intensity from this structure is given by[33]

$$I(q)=\frac{1-C^2}{1-2C\cos\phi+C^2}, \tag{2}$$

where $C=(1-P)\cos(qa_0-\phi)+P\cos(qa_1-\phi)$.

We fit the defect scattering data with Eq. (2) in Fig. 5. First we adjusted the defect length $a_1$ until the fractional peak shift corresponded to the change in the peak width. A

value of $a_1=(1.17\pm0.02)\ a_0$ worked well for all scans, so we fixed it at the rational value $a_1=7/6\ a_0$. The fits in Fig. 5 were made by adjusting the probability $P$ (defect density) and a scale factor. The resulting $P$ values are plotted in Fig. 4(b) and show the same trend as the FWHM and shift from the Lorentzian fits. The probabilities have been multiplied by 2/7 to convert to reciprocal lattice units since $P=1$ yields a peak shift of 2/7 RLU.

The obtained value of $a_1$ corresponds to an apparent projection of the dislocation Burgers vector onto the (100) direction of $a_0/6$. The usual misfit dislocations in GeSi have Burgers vector $a_0/2[110]$, which have a projection $a_0/2$. It is therefore clear that the simplest misfit dislocations are not responsible, but some other extended defect is instead.

Analogous models have been used to describe incommensurate defect structures on surfaces. For example, in the Au(110) surface, shift and broadening of half integer order peaks were attributed to monoatomic steps which interrupted the lattice periodicity.[34] In the Pt(110) surface, peak shifting and broadening as a function of temperature were observed and explained by randomly distributed steps and anti-phase boundaries.[35] In these cases, peak shifting and broadening were also due to the phase shift caused by monoatomic steps. Similar anti-phase boundary effects were seen in the reconstructed Si(113) surface near its disordering phase transition.[36]

## V. SUMMARY AND CONCLUSIONS

A metastable $Si_{0.7}Ge_{0.3}$ film was irradiated with increasing doses of 25 keV $Ga^+$ ions and the strain relaxation was observed using *in situ* x-ray diffraction. The eventual in-plane position of the diffuse peak at the largest dose before amorphization was in good agreement with the prediction of an equilibrium theory.[29,30] Before irradiation, the diffuse scattering was due to thermal vibration or residual point defects. With increasing dose, additional diffuse scattering was observed. By a dimensional argument, it was shown that the defects causing excess diffuse scattering scale like extended defects. There are a few possible candidates for the type of extended defects: one-dimensional (1D) dislocations, two-dimensional (2D) dislocation loops, 2D stacking faults and 3D precipitates. Among these possibilities, dislocation loops produced inside the film upon irradiation are a likely primary source of diffuse component. However, with x-ray diffraction alone, it is not possible to unambiguously identify the nature of these defects. Use of high resolution transmission electron microscopy (HRTEM) could achieve this in a future study. These defects may be a precursor of dislocations that would ultimately relieve the strain of the film. The Hendricks-Teller model fit our data reasonably well and was used to explain shifting and broadening of excess diffuse scattering components. The residual coherent peak is not explained by the Hendricks-Teller model, which oversimplifies the film as a 1D random dislocation array. The ordering influence of the substrate, omitted from this model, would be expected to give rise to a coherent component, as Kaganer *et al.* have already shown.[32]

## ACKNOWLEDGMENTS

The authors thank P. Partyka and R. S. Averback for help with the $Ga^+$ source and for useful discussions. P. Desjardins helped with the interpretation of the RLMs. This work was supported by the U.S. Department of Energy (DOE) under Grant No. DEFG02-96ER45439 and by the Semiconductor Research Corporation. NSLS is supported by the U.S. DOE under Grant No. DE-AC012-76CH00016.

[1] J. C. Bean, in *Silicon MBE*, edited by E. Kasper and J. C. Bean (Chemical Rubber, Boca Raton, FL, 1988), Vol. 2, Chap. 11.
[2] S. S. Iyer, G. L. Patton, J. M. C. Stork, B. S. Meyerson, and D L. Harame, IEEE Trans. Electron Devices **36**, 2943 (1989).
[3] T. Manku and A. Nathan J. Appl. Phys. **72**, 1205 (1993).
[4] T. Mishima, W C. Fredriksz, G. F. A. van der Walle, D. J. Gravesteijn, R. A. van den Heuvel, and A. A. van Gorkum, Appl. Phys. Lett. **57**, 2567 (1990).
[5] F. Schäffler and H. J. Jorke, Appl. Phys. Lett. **58**, 397 (1991).
[6] R. A. Kubiak, E. Basaran, D. W. Smith, A. D. Plews, J. Brighten, S. M. Newstead, P. Phillips, T. E. Whall, and E. H. C. Parker, *Extended Abstracts of the 1993 International Conference on Solid State Devices and Materials*, Makuhari, 1993, p. 237.
[7] S. C. Jain, J. R. Willis, and R. Bullough, Adv. Phys. **39**, 127 (1990).
[8] R. People and J. C. Bean, Appl. Phys. Lett. **49**, 229 (1985).
[9] D. C. Houghton, J. Appl. Phys. **70**, 2136 (1991).
[10] M. R. Sardela, Jr. and G. V. Hansson, Appl. Phys. Lett. **65**, 1442 (1994); J. Vac. Sci. Technol. A **13**, 314 (1995).
[11] R. Hull and J. C. Bean, Crit. Rev. Solid State Mater. Sci. **17**, 507 (1992).
[12] S. Mantl, B. Holländer, W. Jäger, B. Kabius, H. J. Jorke, and E. Kasper, Nucl. Instrum. Methods Phys. Res. B **39**, 405 (1989).
[13] B. T. Chilton, B. J. Robinson, D. A. Thompson, T. E. Jackman, and J.-M. Baribeau, Appl. Phys. Lett. **54**, 2 (1989).
[14] D. C. Paine, D. J. Howard, N. G. Stoffel, and J. H. Horton, J. Mater. Res. **5**, 1023 (1990).
[15] M. Vos, C. Wu, I. V. Mitchell, T. E. Jackman, J.-M. Baribeau, and J. P. McCaffrey, Appl. Phys. Lett. **58**, 951 (1991).
[16] D. J. Eaglesham, J. M. Poate, D. C. Jacobson, M. Cerullo, L. N. Pfeiffer, and K. West, Appl. Phys. Lett. **58**, 523 (1991).
[17] T. E. Haynes and O. W. Holland, Appl. Phys. Lett. **61**, 61 (1992).
[18] M. Vos, C. Wu, I. V. Mitchell, T. E. Jackman, J.-M. Baribeau, and J. P. McCaffrey, Nucl. Instrum. Methods Phys. Res. B **66**, 361 (1992).
[19] G. Bai and M.-A. Nicolet, J. Appl. Phys. **71**, 4227 (1992).
[20] D. Y. C. Lie, A. Vantomme, F. Eisen, M.-A. Nicolet, V. Arbet-Engles, and K. L. Wang, Mater. Res. Soc. Symp. Proc. **262**, (1993).
[21] Q. Lu, M. R. Sardela, Jr., T. R. Bramblett, and J. E. Greene, J. Appl. Phys. **80**, 4458 (1996).
[22] J. C. Bean, L. C. Feldman, A. T. Fiory, S. Nakahara, and I. K. Robinson, J. Vac. Sci. Technol. A **2**, 436 (1984).
[23] E. Kasper, H.-J. Herzog, and H. Kibbel, Appl. Phys. **8**, 199 (1975).
[24] P. F. Fewster, Semicond. Sci. Technol. **8**, 1915 (1993).
[25] H. Heinke, M. O. Möller, D. Hommel, and G. Landwehr, J. Cryst. Growth **135**, 41 (1994).
[26] P. F. Miceli, C. J. Palmstrom, and K. W. Moyers, Appl. Phys. Lett. **58**, 1602 (1991).
[27] K. Huang, Proc. R. Soc. London, Ser. A **190**, 102 (1947).
[28] P. H. Dederichs, J. Phys. F **3**, 471 (1973).
[29] A. Fischer, H. Kuhne, and H. Richter, Phys. Rev. Lett. **73**, 2712 (1994).
[30] C. Kim, I. K. Robinson, J. M. Myoung, K.-H. Shim, M. C. Yoo, and K. Kim, Appl. Phys. Lett. **69**, 2358 (1997).
[31] B. E. Warren, *X-ray Diffraction* (Addison–Wesley, Reading, MA, 1969).
[32] V. M. Kaganer, R. Köhler, M. Schmidbauer, R. Opitz, and B. Jenichen, Phys. Rev. B **55**, 1793 (1997).
[33] S. B. Hendricks and E. Teller, J. Chem. Phys. **10**, 147 (1942).
[34] I. K. Robinson, Phys. Rev. Lett. **50**, 1145 (1983); I. K. Robinson, Y. Kuk, and L. C. Feldman, Phys. Rev. B **29**, 4762 (1984).
[35] I. K. Robinson, E. Vlieg, and K. Kern, Phys. Rev. Lett. **63**, 2578 (1989).
[36] D. L. Abernathy, S. Song, K. I. Blum, R. J. Bigeneau, and S. G. J. Mochrie, Phys. Rev. B **49**, 2691 (1994); D. L. Abernathy, R. J. Birgeneau, K. I. Blum, and S. G. J. Mochrie, Phys. Rev. Lett. **71**, 750 (1993).